Mandana Shaygan, Brent Usher, & Thomas Baumgartl. (2020). Modelling Hydrological Performance of a Bauxite Residue Profile for Deposition Management of a Storage Facility. Water (Basel), 12(1988).

https://doi.org/10.3390/w12071988

water

MDPI

Article

Modelling Hydrological Performance of a Bauxite Residue Profile for Deposition Management of a Storage Facility

Mandana Shaygan [1,*], Brent Usher [2] and Thomas Baumgartl [3]

[1] Centre for Water in the Minerals Industry, Sustainable Minerals Institute, The University of Queensland, Brisbane, QLD 4072, Australia
[2] Klohn Crippen Berger Ltd., Brisbane, QLD 4101, Australia; BUsher@klohn.com
[3] Geotechnical and Hydrological Engineering Research Group, Federation University, Churchill, VIC 3841, Australia; t.baumgartl@federation.edu.au
* Correspondence: m.shaygan@uq.edu.au

Received: 15 May 2020; Accepted: 9 July 2020; Published: 14 July 2020

Abstract: Accurate scheduling of bauxite residue (red mud) deposition time is required in order to prevent the risk of storage facility failure. This study was conducted to precisely determine the hydraulic parameters of bauxite residue and investigate the capability of HYDRUS to accurately estimate the residue moisture profile and the timing for its deposition. The hydraulic properties of the bauxite residue profile were determined by solving an inverse problem. A one-dimensional hydrological model (HYDRUS-1D) was validated using a 300 mm long column filled with bauxite residue and exposed to a dynamic lower boundary condition. After numerical validation, the model was used to simulate the moisture profile of bauxite residue under the climatic conditions of an alumina refinery site in Queensland, Australia, as well as other scenarios (i.e., high (300 mm) and small (1.7 mm) rainfall events of the site). This study showed that the HYDRUS model can be used as a predictive tool to precisely estimate the moisture profile of the bauxite residue and that the timing for the re-deposition of the bauxite residue can be estimated by understanding the moisture profile and desired shear strength of the residue. This study revealed that the examined bauxite residue approaches field capacity (water potential −10 kPa) after three days from a low rainfall event (<1.7 mm) and after eight days from an intense rainfall event (300 mm) at the time of disposal. This suggests that the bauxite residue can be deposited every four days after low rainfall events (as low as 1.7 mm) and every nine days after high rainfall events (as high as 300 mm) at the time of deposition, if bauxite residue experiences an initial drying period following deposition.

Keywords: bauxite residue hydraulic parameters; HYDRUS; inverse modelling; moisture content; red mud; shear strength

1. Introduction

Bauxite residue is a caustic and high alkaline by-product of the Bayer process, where bauxite ore (aluminium containing mineral) is digested with high concentrations of NaOH (sodium hydroxide) under high pressure and heat to produce alumina, raw material for the production of aluminium [1–3]. Bauxite residue production can fluctuate from 0.3 to 2.5 tonnes per tonne of alumina produced, and as the utilization of bauxite residue is low, the majority of the material is discharged into a storage facility [4]. Dry stacking is currently the main method for bauxite residue disposal, in which the bauxite residue typically discharges into a storage facility in layers up to 500 mm deep and is allowed to dry via evaporation [1]. The bauxite residue is also cultivated periodically using amphirolling to assist with dewatering [5–7]. Some refineries deposit the residue as paste slurry [7]. In some refineries,

the residue is filtered (vacuum filtration) [8,9] or treated by thickeners [10,11] to increase the solid content prior to disposal. In a storage facility, the stored residue is not covered with fresh residue until it has reached its target dryness (approximately 70%) [1,12]. Therefore, estimating the bauxite residue moisture profile is essential to guarantee the continuous and safe disposal of the bauxite residue into a storage area, since the continuous placement of the bauxite residue in a storage facility with a high moisture content can increase the risk of a storage facility failure [13].

Numerical modelling is a meaningful tool to evaluate and forecast water movement within porous media [14,15]. It can also predict the effects of long-term climatic conditions on moisture fluctuations within porous media [16–18]. Therefore, a hydrological model may assist with the estimation of the bauxite residue moisture profile, leading to the scheduling of the disposal time for the bauxite residue. Numerical models (e.g., HYDRUS) which consider the detailed knowledge of pore systems and hydraulic parameters should be used for the estimation of the moisture profile. However, the applicability of a soil hydrological model to estimate the moisture profile of bauxite residue in a storage facility has not been assessed.

Bauxite residue is characterised by very fine textured material and very high salinity, resulting in a much reduced drainage capacity and leading to prolonged times for drying and stabilising the substrate. The bauxite residue moisture profile and its drying behaviour are determined directly by the hydrological parameters, which are bauxite residue/site specific. Likewise, the mineralogy and chemical composition of bauxite residues are affected by both the impurities present in each bauxite ore and the different Bayer process conditions of each individual refinery [19]. Hence, generalised assumptions of bauxite residue's hydrological properties from each refinery may be misleading, and an individual site material characterisation is needed. The soil water retention characteristics, one of the main hydrological properties, are typically obtained by laboratory experiments, using porous media-based methods such as the sand box, pressure cells and pressure plate extractors [20]. Tension disc infiltrometers allow field based in-situ measurements [21–25]. However, the bauxite residue's hydraulic parameters are difficult to measure in a laboratory due to its shrinkage behaviour [26]. Using a tension disc infiltrometer for deriving water retention characteristics is limited because of the continuous placement of the residue into a storage facility and the inaccessibility of the site. Thus, an indirect approach has been chosen for determining the bauxite residue's hydrological properties by approaching the case as an inverse problem.

This study aims to (i) evaluate the effectiveness of inverse modelling in determining bauxite residue's water retention characteristics, (ii) investigate the capability of a numerical hydrological model to simulate a bauxite residue moisture profile and (iii) estimate the surface moisture profile of bauxite residue for the purpose of scheduling the deposition of bauxite residue in a storage facility.

2. Materials and Methods

2.1. Determining Physical Properties of Bauxite Residue

Bauxite residue (EC: 20.03 ± 0.05 dS m^{-1}; pH: 8.64 ± 0.04; Hematite: 82%; Halite: 6%; Anastase: 2%; Quartz: 2%; Sodalite: 8%) was collected from a bauxite residue storage facility in North Queensland, Australia (23°56′4.81″ S and 151°18′59.51″ E). The particle size distribution of the bauxite residue was determined using Malvern Mastersizer 3000 (Malvern Panalytical Ltd.; Malvern, Worcestershire, UK).

The collected bauxite residue was dried in a 40 °C dehydrating oven and sieved to <2 mm. This created micro-aggregates (<200 µm). The sieved bauxite residue was then packed into three small cores (40 mm height and 56 mm diameter) to the bulk density of 0.9 ± 0.02 Mg m^{-3}. The bulk density of bauxite residue was low due to the high particle density (2.85 Mg m^{-3}) and uniform particle size. The cores were then saturated with DI water (deionised water) from the bottom of the core, with the intention of achieving no drainage or off-flow of pore solution from the samples. The saturated cores were then used to determine the water retention characteristics and hydraulic conductivity of bauxite residue, as described in Shaygan et al. [27]. To measure the water retention curve, the bauxite residue

cores were desiccated to −1, −2 and −3 kPa for 24 h, each using a sand-based tension table. Vacuum controlled pressure was used to achieve a lower water potential; the bauxite residue cores were placed on a porous plate for 4 days and 6 days sequentially, in order to obtain water content at an equilibrium with the water potential at −10 and −30 kPa. The desiccation at the equivalent of −500 kPa was applied using a pressure plate extractor (1500F1; Soil Moisture; Santa Barbara, CA, USA) for 3 weeks. The cores were weighed to determine the gravimetric water content for each desiccation step. The volumetric water content of each step was then calculated using the bulk density of the cores. Subsequently, the water retention curve (parameters of van Genuchten equation [28]) of the residue was determined based on the measured data by using RETC software [29].

The saturated hydraulic conductivity of the bauxite residue was measured using a constant head permeability test [30]. The hydraulic conductivity procedure test followed the method described in Shaygan et al. [27]. DI water was applied to the columns from the bottom of the bauxite residue cores, and the volume of water passing through the cores was determined in order to calculate the flow rate and, hence, the hydraulic conductivity, based on Darcy's law [31]. The saturated hydraulic conductivity and water retention characteristics curve were measured for the same bauxite residue cores. The detailed hydrological properties of bauxite residue are presented in Table 1.

Table 1. Hydrological properties of the bauxite residue.

Parameters	θs (cm^3 cm^{-3})	θr (cm^3 cm^{-3})	α (cm^{-1})	n	K_{sat} (cm s^{-1})	Sand (%)	Silt (%)	Clay (%)
(n = 3)	0.651 ± 0.01	0.336 ± 0.02	0.0356 ± 0.0007	1.384 ± 0.02	$5.82 \times 10^{-5} \pm 0.2 \times 10^{-5}$	4 ± 0.5	43 ± 1.02	53 ± 1.12

Average value ± standard deviation; α: inverse of the air entry suction; n: measure of the pore size distribution; θs: saturated water content; θr: residual water content; K_{sat}: saturated hydraulic conductivity; n: number of samples

A Wille Geotechnik automatic vane shear tester (Wille Geotechnik GmbH, Göttingen, Germany) was used to obtain the vane shear strength of the bauxite residue samples approximately at the liquid limit (63% gravimetric water content) and after approaching field capacity. The vane used for the experiment had a 25.4 mm height and 12.7 mm diameter. The vane shear testing was carried out at a rotation rate of 6°/min.

2.2. Laboratory Column Study

A series of laboratory column studies was conducted to observe the moisture fluctuations within a bauxite residue profile. The dried bauxite residue (<2 mm) was packed into a 300 mm long column (diameter 70 mm) to the bulk density of 0.9 Mg m^{-3} ± 0.02 (Figure 1). The column was subjected to three wet–dry cycles to approximate advanced consolidation after refilling, in which the column was moistened by DI water from the bottom of the columns for 24 h and then allowed to dry for 7 days in a 40 °C dehydrating oven. The bottom of the column was enclosed to avoid any changes in the water mass balance of the column. Following the last cycle, the column was saturated. The experiment was then conducted by enclosing the top of the column to avoid evaporation and "gradually" establishing a water potential of −6 kPa for the bauxite residue surface by collecting outflow (Figure 1). This experiment was used for the validation of the HYDRUS model. A separate experiment, similar to the above set up, was also conducted for inverse modelling. However, for this experiment, the water potential of −6 kPa for the bauxite residue surface was established by placing the outflow at 300 mm below the lower end of the column and collecting the outflow (Figure A1). For both experiments, the hydrological response in the columns was monitored by measuring the water potential using tensiometers (T5x; UMS; Munich, Germany), which were installed at three depths (35, 120 and 250 mm). The water potentials were measured at one-minute intervals. Similarly to small cores (40 mm height and 56 mm diameter), no changes were observed in the structure or volume of the bauxite residue during the column studies.

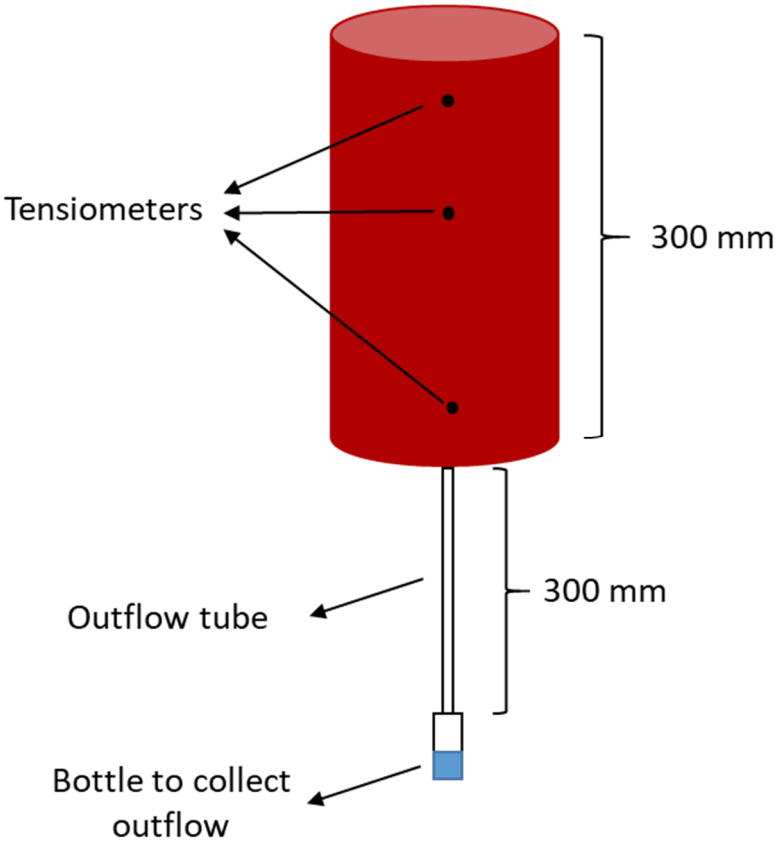

Figure 1. Schematic model of column study.

2.3. Inverse Solution Modelling

Packing disturbed material into a different size volume (here, a column of 300 mm height and 70 mm diameter) can modify the parameters of the water retention characteristics curve [14,16,32,33]. Therefore, the hydraulic parameters of the bauxite residue were optimised separately for the larger test column. An inverse solution was used to optimise the bauxite residue's hydraulic parameters (parameters of water retention curve (Equation (1)) and the hydraulic conductivity curve (Equation (2)), in which the parameters of three depths (35, 120 and 250 mm) were optimised simultaneously.

$$\theta_{(\Psi)} = \theta_r + \frac{\theta_s - \theta_r}{[1 + (\alpha|\Psi|)^n]^{1-1/n}} \quad (1)$$

$$K(h) = K_s\, S_e^l \left[1 - \left(1 - S_e^{1/\left(1-\frac{1}{n}\right)}\right)^{1-1/n}\right]^2 \quad (2)$$

where $\theta_{(\Psi)}$ is the water content ($L^3\ L^{-3}$); $|\Psi|$ is the suction pressure (L); θs is the saturated water content ($L^3\ L^{-3}$); θr is the residual water content ($L^3\ L^{-3}$); α is the inverse of the air entry suction (L^{-1}); n is the gradient of the water retention curve and reflects the pore size distribution characteristic; S_e is the effective water content; K_s is the saturated hydraulic conductivity ($L\ T^{-1}$); $K(h)$ is the unsaturated hydraulic conductivity at the pressure head ($L\ T^{-1}$).

In this study, the Marquart–Levenberg method was used [34] to solve the inverse problem through HYDRUS, as described in Šimůnek et al. [35]. The aim of the inverse modelling was to generate

van Genuchten parameters, which minimise the difference between simulated and observed water potentials through an objective function, Φ, which is defined as

$$\Phi(b,p) = \sum_{j=1}^{m} \sum_{i=1}^{nj} \left[P_{ij}^{*} - P_{ij}(b) \right]^2 \quad (3)$$

where m is two types of datasets (observed pressure heads and total water volumes in the sample), n_j represents the number of measurements in a particular measurement set, P_{ij}^{*} and $P_{ij}(b)$ are the observations and predictions in a particular measurement set, and b is the vector of optimised parameters (e.g., α, n, θs, θr and K_{sat}). As part of the inverse solution, HYDRUS generated a correlation matrix-specified degree of correlation between the fitted coefficients. HYDRUS also provided some statistical information about the fitted parameters, such as the lower and upper confidence limits (Table A1).

The same initial and boundary conditions as the laboratory column study were defined in the inverse modelling. The measured hydraulic parameters from small cores (Table 1) were used as initial inputs for the inverse modelling. The number of observations for each depth was 1500. During the procedure, the hydraulic functions were optimised so that the observed and predicted values for the actual outflow, as well as water potentials in three depths, were as close as achievable. Then, the performance of the inverse solution was evaluated using statistical analyses. The final optimised hydraulic functions of the bauxite residue are presented in Table 2.

Table 2. HYDRUS model inputs for simulation of the bauxite residue moisture profile.

Parameter	Value
Hydraulic parameters	
Saturated hydraulic conductivity (K_{sat}), cm s^{-1}	5.66×10^{-5}
Residual volumetric water content (θr), cm^3 cm^{-3}	0.2 ǂ
Saturated volumetric water content (θs), cm^3 cm^{-3}	0.699 ǂ
Inverse of air entry suction α, cm^{-1}	0.001 ǂ
Measure of the pore size distribution n	1.14 ǂ
Pore connectivity parameter l	0.5
Discretisation	
Grid spacing, cm	0.1
Initial time step, second	0.006
Min. time step, second	0.0012
Max. time step, second	60

ǂ optimised parameters using inverse solution.

2.4. Validation of HYDRUS Model

Water potential fluctuations on a laboratory scale were simulated using HYDRUS-1D (version 4.16.0110) [36]. The results from the laboratory column study were compared with the HYDRUS-1D modelling results for validation of the model. The number of observations for each depth was 12,701. The components of the HYDRUS-1D model which were applicable for this study are described comprehensively in Šimůnek et al. [36] and Šimůnek et al. [34]. To validate the HYDRUS model, the numerical mesh of a 300 mm long column was generated. The single porosity model and the van Genuchten–Mualem model were chosen for describing the hydraulic functions. The final optimised hydraulic functions of van Genuchten–Mualem (Table 2) of the bauxite residue were used for the validation. Variable pressure head conditions were applied as upper and lower boundary conditions for the model. Then, the model validation was confirmed using statistical analyses.

2.5. Statistical Analyses

To evaluate the performance of inverse modelling and the validation of HYDRUS, the observed data were compared with the simulated data using the following statistical analyses:

The root means square error (*RMSE*), which is defined as [37,38]:

$$RMSE = \sqrt{\frac{\sum_{i=1}^{N}(Pi - Oi)^2}{N}} \tag{4}$$

The Nash–Sutcliffe coefficient *(NSE)*, which is a goodness-of-fit measure [14,39]:

$$NSE = 1 - \frac{\sum_{i=1}^{N}(Oi - Pi)^2}{\sum_{i=1}^{N}\left(Oi - \overline{O}\right)^2} \tag{5}$$

The index of agreement (*d*), which is defined as [40]:

$$d = 1 - \frac{\sum_{i=1}^{N}(Oi - Pi)^2}{\sum_{i=1}^{N}\left(\left|Pi - \overline{O}\right| + \left|Oi - \overline{O}\right|\right)^2} \tag{6}$$

where

$$\overline{O} = \frac{1}{N}\sum Oi \tag{7}$$

where *Oi* and *Pi* are observed and simulated values, and *N* is the number of observations. The model is more accurate when the *RMSE* is closer to zero [38] and the *NSE* and index of agreement (*d*) are closer to one [39,40].

2.6. Simulation of Bauxite Residue Moisture Profile Using HYDRUS

Following the validation of the model, the water potential of bauxite residue within a storage facility was simulated for a period of over 11 years (2007–2018), using the climatic conditions of the study site (Figure 2). In a bauxite residue storage facility, lateral water movement within the profile is negligible due to a very low hydraulic conductivity. Therefore, the choice of the HYDRUS-1D model is deemed applicable for the simulation of the bauxite residue moisture profile.

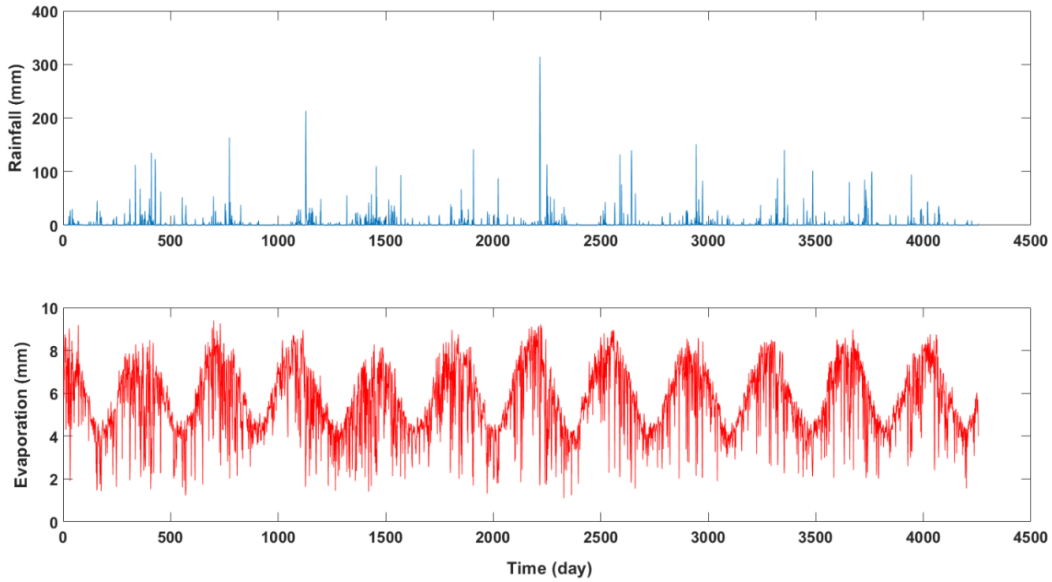

Figure 2. Rainfall and evaporation series of the studied site.

A profile with a 2000 mm depth was selected for this simulation study to define a lower boundary condition that is deep enough not to be directly affected by the evaporation. The single porosity model and the van Genuchten–Mualem model were applicable for this study based on the validation study, and thus the final optimised hydraulic parameters (Table 2) were used for the simulation. Atmospheric boundary conditions with surface runoff and no flux, which reflected the storage facility boundary conditions, were chosen for the upper and lower boundary conditions of the model, respectively. Different initial pressure heads (−1 kPa, −2 kPa and −10 kPa) were applied to the model in order to best reveal the conditions of the storage facility from near saturation up to approximate field capacity condition for the bauxite residue farming stage (creating ridges by an amphibious scrolling tractor within the surface of the bauxite residue to increase evaporation [7]). The rainfall and potential evaporation of the storage facility site (Figure 2) were applied to the model. The model then simulated the moisture profile for a period of 4256 days under the natural climatic conditions of the site, as well as for selected scenarios with small (1.7 mm) and high (300 mm) rainfall events at the time of deposition.

3. Results and Discussion

3.1. Evaluating the Performance of Inverse Modelling

The index of agreement values between the observed and simulated data (number of observations: 1500) for inverse modelling were greater than 0.96 for all studied depths (Table 3). The NSE values, which inform the goodness of fit, were also greater than 0.82 and close to one, while the RMSE values were less than 0.34 and close to zero (Table 3). All the above suggested that the inverse solution technique successfully determined the hydraulic functions of the bauxite residue profile. The bauxite residue had a high air entry value (Table 2) as it is a very fine textured material (Table 1). The chemistry of bauxite residue, particularly given the type and quantity of iron minerals (i.e., goethite and hematite), can also affect the hydraulic parameters of the material, as well as the mechanical behaviour of bauxite residue [19]. In this study, the inverse modelling overestimated (0.69 cm^3 cm^{-3}) the measured saturated water content (0.65 cm^3 cm^{-3}), while the estimated residual water content (0.2 cm^3 cm^{-3}) was found to be lower than the measured residual water content (0.33 cm^3 cm^{-3}) (Tables 1 and 2). In agreement with other studies [41–43] which indicated that inverse modelling overestimates the total porosity, a smaller measured saturated water content could possibly be explained by the incomplete saturation and air entrapment of the bauxite residue in the laboratory. Interestingly, the estimated saturated hydraulic conductivity (5.66×10^{-5} cm s^{-1}) of bauxite residue was comparable to the measured hydraulic conductivity (5.82×10^{-5} cm s^{-1}) (Tables 1 and 2), and this confirms the closeness of inverse modelling in estimating the value of the saturated hydraulic conductivity.

Table 3. Statistical comparison of observed and simulated data for evaluation of inverse modelling.

Statistical Analyses	Depth of the Bauxite Residue Profile		
	35 mm	**120 mm**	**250 mm**
RMSE (n = 1500)	0.3050	0.3475	0.1936
NSE (n = 1500)	0.8887	0.8215	0.8895
d (n = 1500)	0.9766	0.9609	0.9757

n: number of observations; *RMSE*: root mean square error; *NSE*: Nash–Sutcliffe coefficient; *d*: index of agreement.

3.2. Investigating HYDRUS-1D's Capability as a Predictive Tool for Estimating Bauxite Residue Moisture Profile

After optimizing the hydraulic parameters using inverse modelling, the performance of the HYDRUS model for estimating the moisture profile of bauxite residue was investigated using the large data series (number of observation: 12701) obtained from the column study and by statistical analyses (Figure 3 and Table 4). In this study, the NSE values ranged between 0.92 and 0.99 across different depths of the bauxite profile (Figure 3 and Table 4). The simulation also reflected the observed

water potential values (d > 0.98) at different depths of the bauxite profile, and the RMSE values were very small for all studied depths (Figure 3 and Table 4). Therefore, this study showed that the observed and simulated water potentials correlate very well for all studied depths of the bauxite residue profile. Similar to studies on soil [14,16–18,44,45], tailings [46,47] and waste rocks [48–50] that indicated that HYDRUS reproduces the dynamics of moisture content in porous media, this study suggested that HYDRUS can precisely simulate the water potential of bauxite residue for drying events to high satisfaction.

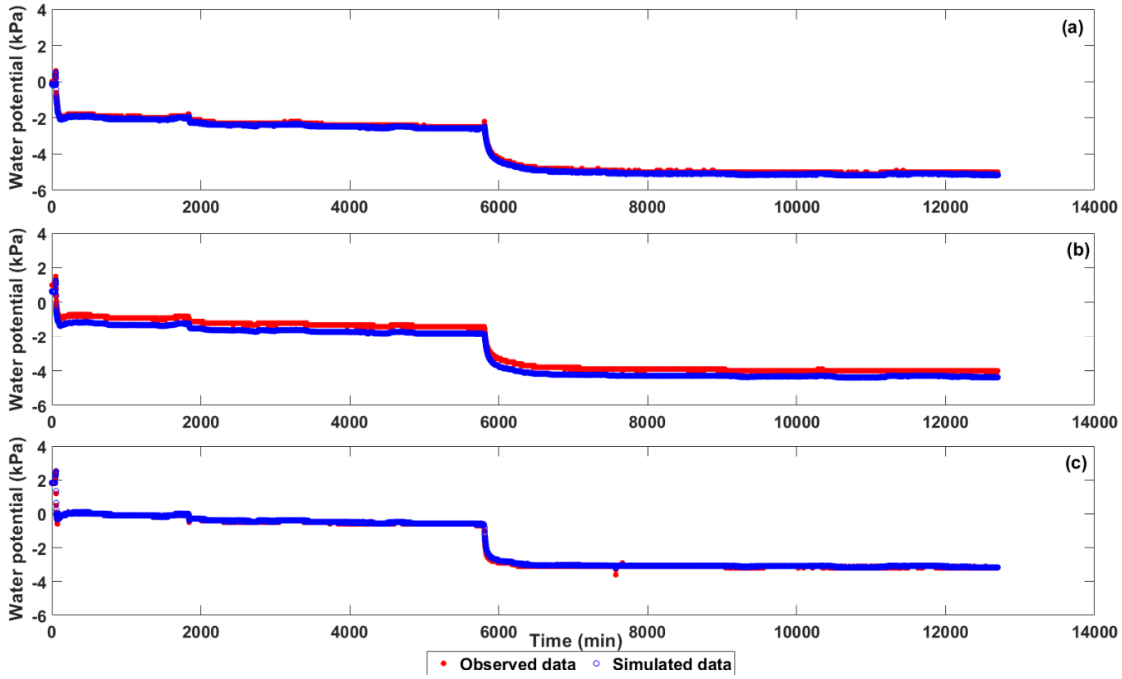

Figure 3. Observed and simulated bauxite residue water potential at depths of (**a**) 35 mm, (**b**) 120 mm and (**c**) 250 mm.

Table 4. Statistical comparison of observed and simulated data for validation of the model.

Statistical Analyses	Depth of the Bauxite Residue Profile		
	35 mm	120 mm	250 mm
RMSE (n = 12,701)	0.08	0.37	0.04
NSE (n = 12,701)	0.99	0.92	0.99
d (n = 12,701)	0.99	0.98	0.99

n: number of observations; *RMSE*: root mean square error; *NSE*: Nash–Sutcliffe coefficient; *d*: index of agreement.

3.3. Application of HYDRUS-1D Modelling for Management of a Bauxite Residue Storage Facility

After validation of the model, HYDRUS was used to simulate the bauxite residue moisture profile in a storage facility under the natural climatic conditions of the site and based on scenarios related to the deposition of bauxite residue into a storage facility (i.e., different initial water potential from near saturation to water contents similar at the condition of bauxite residue farming). Firstly, the validated model was run for 4256 days, and the simulated water potential values were shown to a depth of 100 cm under the studied climatic scenario (Figure 4). In this study, the pF value (logarithm of negative water potential (hPa)) was chosen to present the simulated data in order to more clearly depict the moisture conditions at a wetter state, which is of higher relevance for the interpretation of the simulated data.

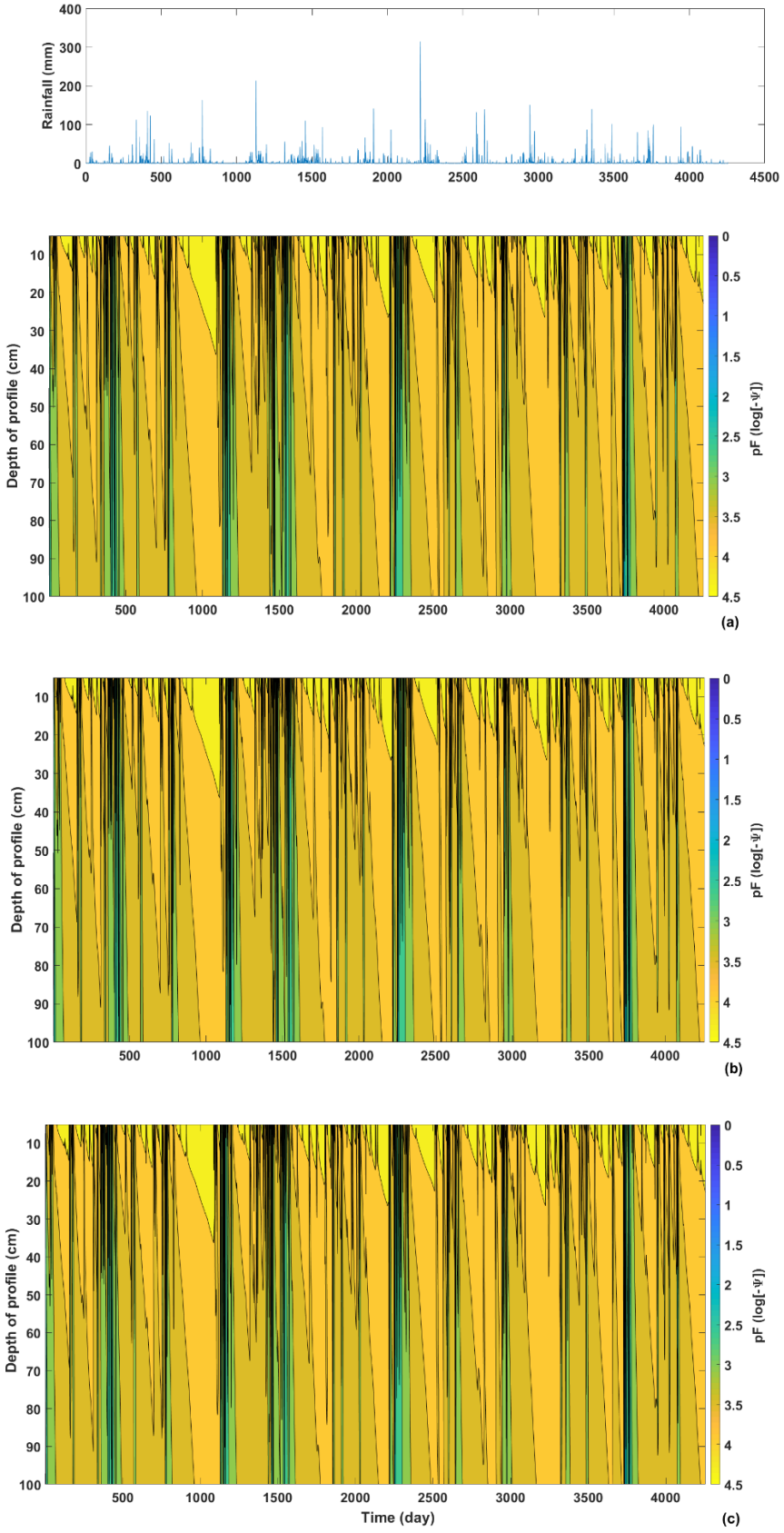

Figure 4. The simulated water potentials of the bauxite residue in a storage facility with initial water potentials of (**a**) −1 kPa, (**b**) −2 kPa and (**c**) −10 kPa. Ψ: water potential (hPa).

Fluctuations in the moisture content of the profile were mostly observed up to a depth of 10 cm, and intense rainfall events only influenced the moisture content of the bauxite residue in the greater depths of the profile (Figure 4). Interestingly, the moisture profiles were similar during long-term simulations (4256 days), irrespective of their initial water content, and except for when the intense rain events occurred, the profiles had very low (negative) water potentials, between −100 kPa (pF: 3) and −3000 kPa (pF: 4.5) (Figure 4). The water potential exceeded −1000 kPa (pF: 4) during long-term drought conditions (lack of intense rainfall events) (Figure 4). In this context, Wissmeier et al. [51] reported that the water potential of residue sand obtained from bauxite residue did not drop below −1500 kPa (pF: 4.17) during drought conditions (periods with lack of sufficient rainfall). In our study, the high clay and silt content of the bauxite residue (i.e., fine texture of bauxite residue) affected its hydraulic parameters (i.e., high residual water content and low hydraulic conductivity) (Tables 1 and 2), and thus led to the low infiltration of water to deeper depths of the profiles. The fine texture of bauxite residue also caused bauxite residues with different initial water potentials to display similar moisture profiles. The high amount of simulated runoff (2416 mm), resulting from bauxite residue's low hydraulic conductivity, further contributed to the comparable moisture profiles of the bauxite residue with different initial moisture content levels, from near saturation up to field capacity at the time of deposition (Table 5).

Table 5. The simulated water balance parameters.

Initial Water Potential Content	Cumulative Run-Off (mm)	Cumulative Evaporation (mm)	Cumulative Rainfall (mm)	Cumulative Drainage (mm)	Water Balance Error (%)
−1 kPa	2416.6	10,416	12,765.5	0.0001	0.057
−2 kPa	2416.6	10,415	12,765.5	0.0001	0.056
−10 kPa	2416.3	10,410	12,765.5	0.0004	0.048

Prediction of the bauxite residue moisture profile using HYDRUS can assist with scheduling deposition time in a storage facility, in which by understanding the moisture profile (Figures 5 and 6) and the desired shear strength of the bauxite residue, the re-deposition time into the storage facility can be predicted. Similar to soil [52], there is a relationship between the moisture content and shear strength of bauxite residue, in which bauxite residue with a decreasing water content creates increasing shear strengths (Figure 7). By linking hydrological information with geomechanical properties, it is possible to calculate the required shear strength in a storage facility. This can be achieved by allowing a decrease in water potential through drying, which is equivalent to achieving a certain moisture content distribution of the bauxite residue profile. Hence, scenario modelling using a hydrological model (here, HYDRUS) and linking to geomechanical processes can assist with improving the scheduling of the disposal.

The validated model was re-run, with 1.7 mm and 300 mm rainfall events representing small and intense rainfall events at the study site, respectively (Figure 2), on the day of deposition. The simulation with 1.7 mm rain showed that the bauxite residue profiles approached −10 kPa (pF: 2) after three days (Figure 5). In the case of a high rainfall event (i.e., 300 mm rain in one day) at the time of deposition, the water potentials of the bauxite residues approached −10 kPa (pF: 2) after eight days, irrespective of the initial moisture content (Figure 6). Therefore, if field capacity (−10 kPa) (Table 1) with 19.56 kN m^{-2} shear strength (Figure 7) could provide a safe/suitable condition for the deposition of the residue (in terms of consolidation), this study suggests that the bauxite residue can be deposited onto previously-placed residue (in a storage facility) at intervals of four days under low rainfall event conditions and with a cycling time of nine days following an intense rainfall event (as high as 300 mm), provided that the bauxite residue experiences a period of drying after the rainfall event. These findings can be generalized to bauxite residues with similar properties that are stored under comparable climatic conditions. Finally, the application of the results for management purposes depends largely on the decision criteria for an acceptable or required depth of drying prior to the re-deposition of bauxite residue.

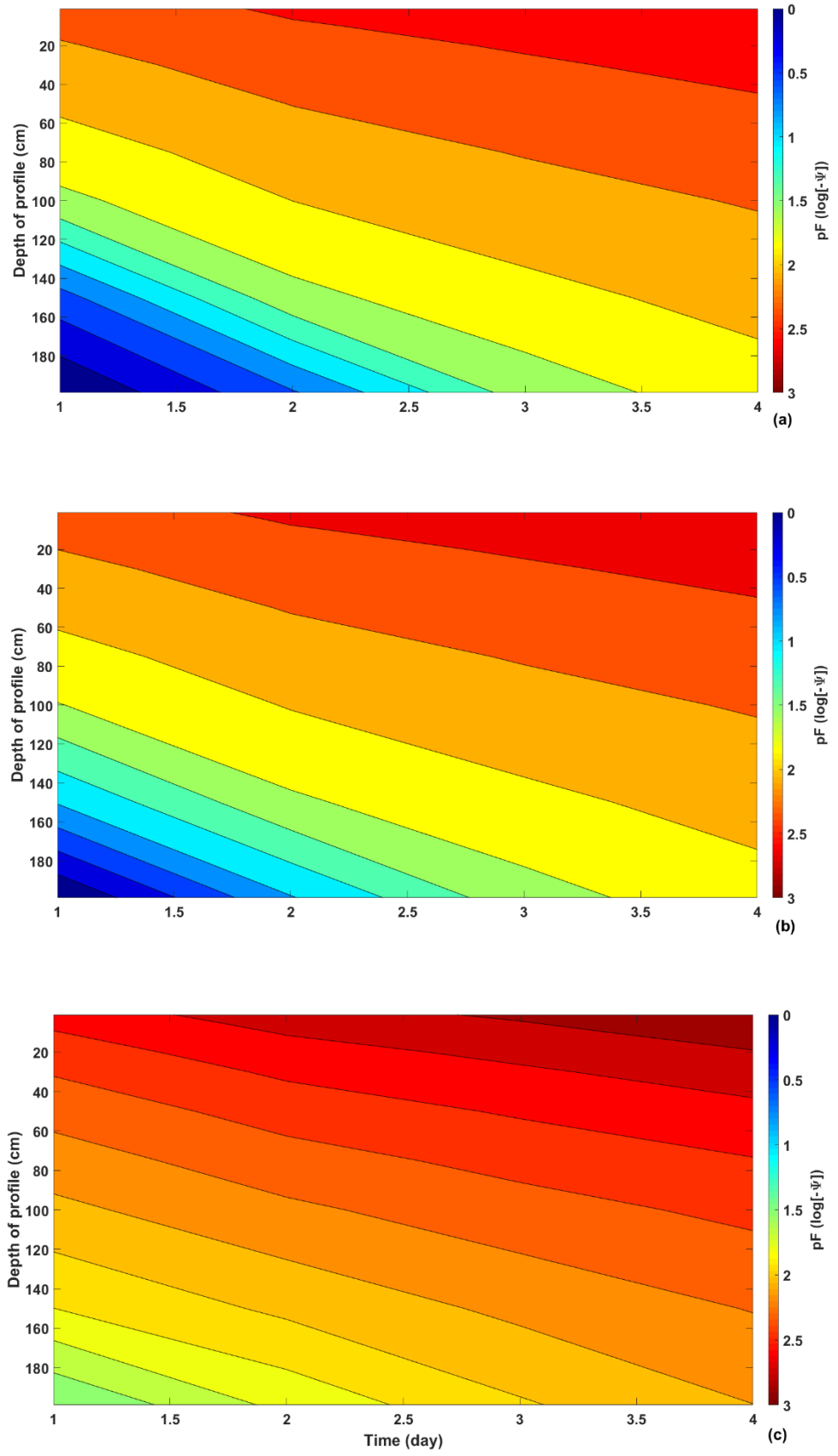

Figure 5. The simulated water potentials of the bauxite residue in a storage facility with initial water potentials of (**a**) −1 kPa, (**b**) −2 kPa and (**c**) −10 kPa when exposed to a small rainfall event (1.7 mm). Ψ: water potential (hPa).

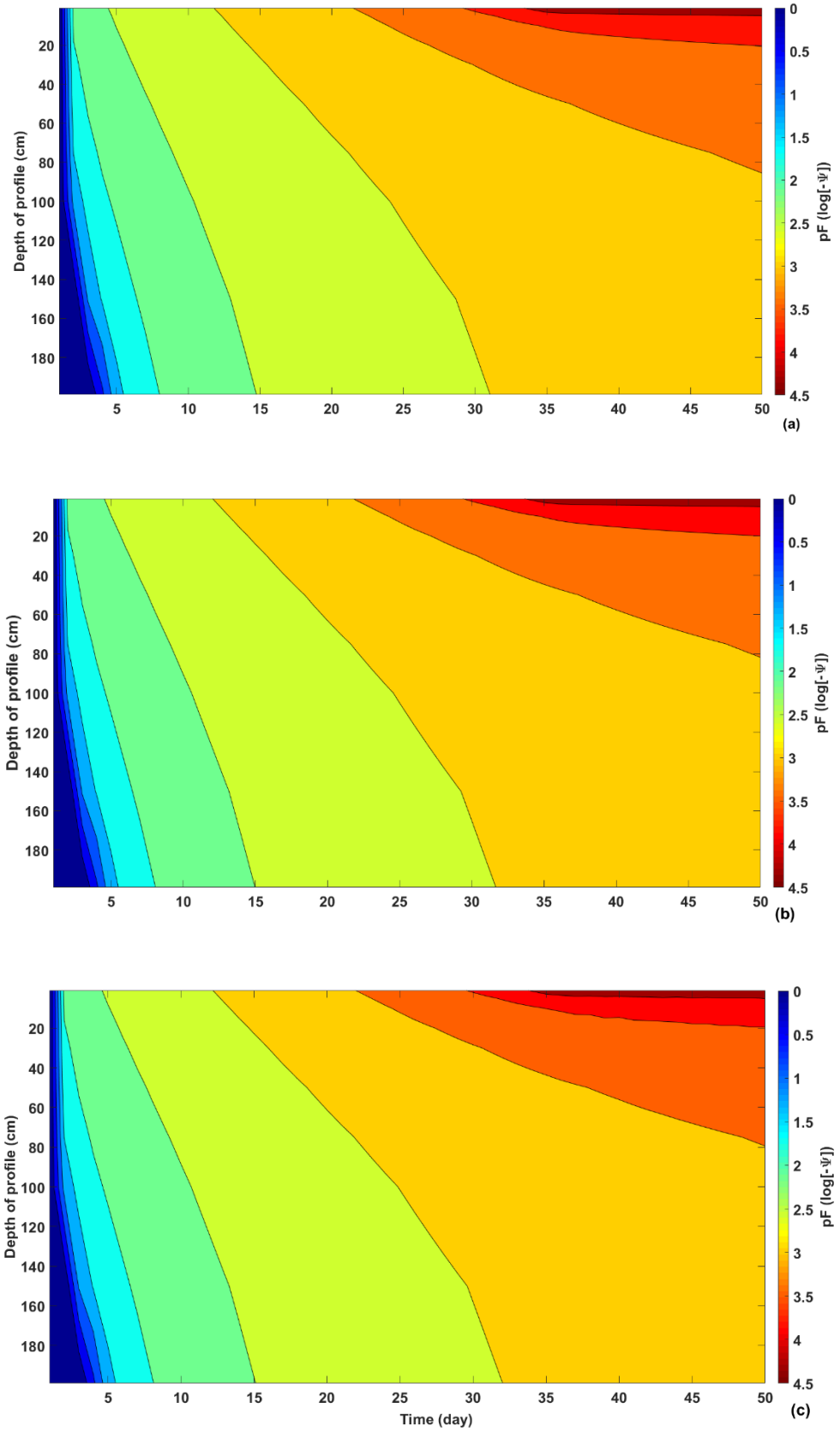

Figure 6. The simulated water potentials of the bauxite residue in a storage facility with initial water potentials of (**a**) −1 kPa, (**b**) −2 kPa and (**c**) −10 kPa when exposed to an intense rainfall event (300 mm rainfall event). Ψ: water potential (hPa).

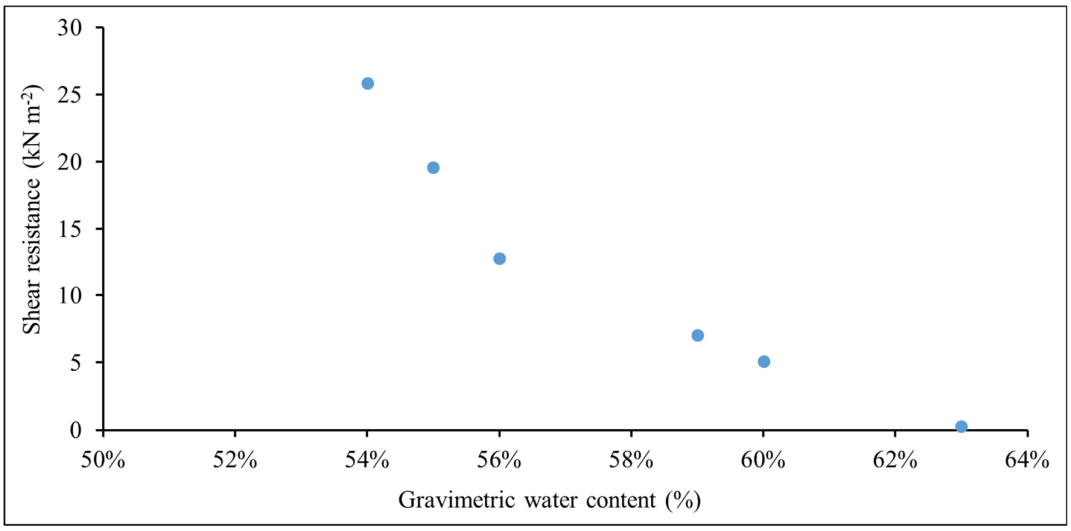

Figure 7. Vane shear strength of the bauxite residue versus its gravimetric water content.

4. Conclusions

The timing for the disposal of bauxite residue into a storage facility is of critical consideration for an efficient refinery operation, land usage, and in order to minimize environmental hazards (i.e., tailings dam failure). This study successfully derived the water retention characteristics of bauxite residue and showed that the time for re-deposition of the bauxite residue into the storage facility can be estimated by numerical simulation techniques (here, the HYDRUS-1D model) based on the simulated moisture profile of the bauxite residue and the desired shear strength. The simulation of the moisture profile of the investigated and pre-treated bauxite residue suggests that the bauxite residue can be deposited into a storage facility every four days if the amount of rainfall is low (<1.7 mm). The modelling study also suggests that the extent of rewetting of the bauxite residue depth profile following an intense rainfall event (300 mm) can delay the deposition of fresh bauxite residue to nine days. While these results are promising, the application of the model requires care, as the salinity of the bauxite residue may reduce the evaporation and delay desiccation.

Author Contributions: Conceptualization, M.S. and T.B.; methodology, M.S.; software, M.S.; validation, M.S.; formal analysis, M.S.; investigation, M.S. and T.B.; resources, M.S., T.B. and B.U.; data curation, M.S. and T.B.; visualization, M.S.; writing—original draft preparation, M.S.; writing—review and editing, M.S., T.B. and B.U.; project administration, M.S., B.U. and T.B. All authors have read and agreed to the published version of the manuscript

Funding: This research was funded by Klohn Crippen Berger Ltd., grant number RM2017002303.

Acknowledgments: The authors would like to thank the Centre for Mined Land Rehabilitation and the Centre for Water in the Minerals Industry for providing the laboratory facility to conduct this research.

Conflicts of Interest: The authors declare no conflict of interest.

Appendix A

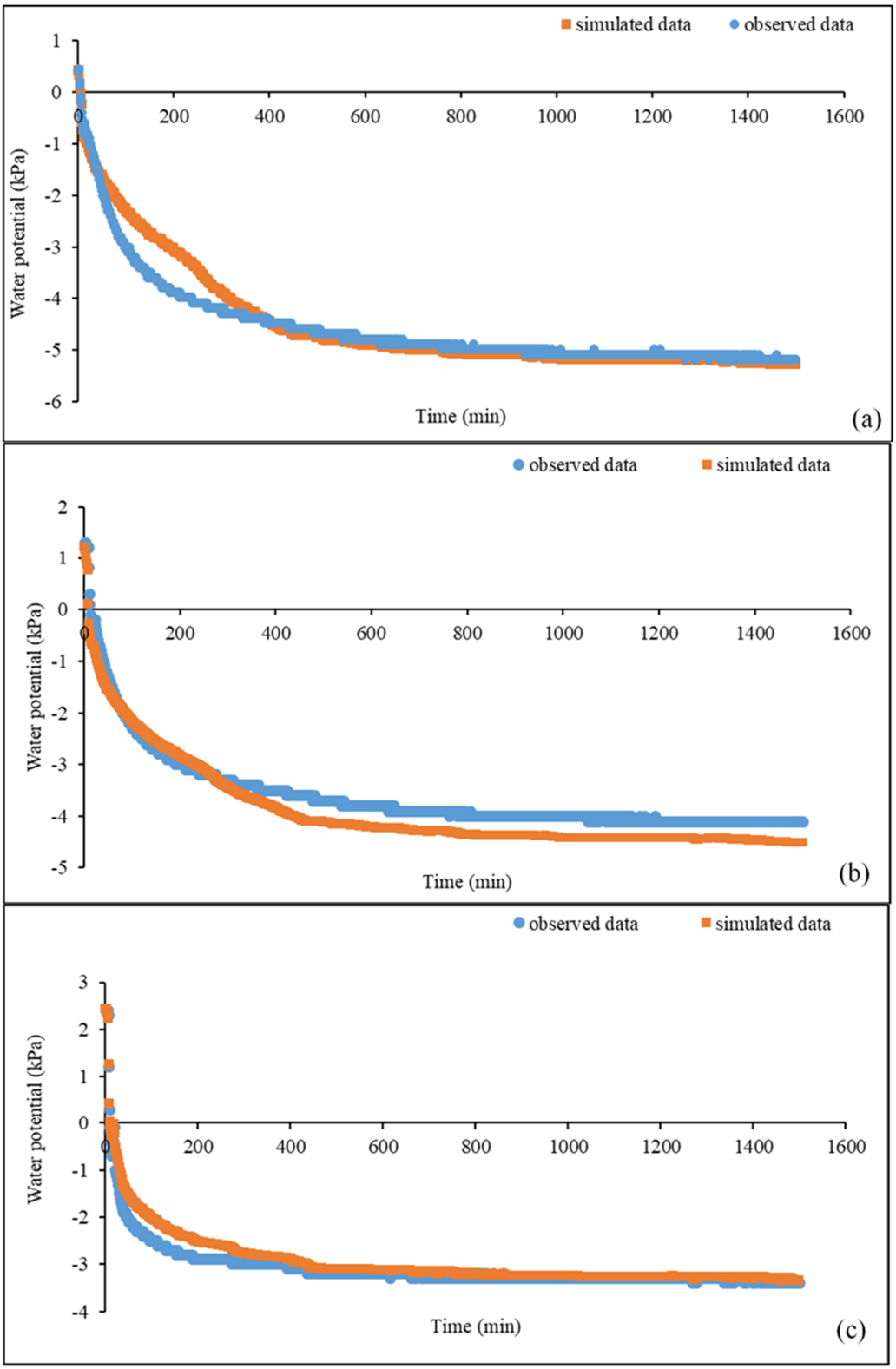

Figure A1. The visual comparison between the observed and simulated water potential values for inverse modelling at the depth of (**a**) 35 mm, (**b**) 120 mm and (**c**) 250 mm.

Table A1. The lower and upper confidence limits for optimized parameters in inverse modelling.

Variable	Limit of Confidence at 95%	
WCR	−3.013	3.428
WCS	−3.120	4.520
α	−0.0033	0.0053
n	0.559	2.241

WCR: residual volumetric water content (cm^3 cm^{-3}); WCS: saturated volumetric water content (cm^3 cm^{-3}); α: inverse of air entry value (cm^{-1}); n: fitting parameter.

References

1. Jones, B.E.H.; Haynes, R.J. Bauxite processing residue: A critical review of its formation, properties, storage, and revegetation. *Crit. Rev. Environ. Sci. Technol.* **2011**, *41*, 271–315. [CrossRef]
2. Gräfe, M.; Power, G.; Klauber, C. Bauxite residue issues: III. Alkalinity and associated chemistry. *Hydrometallurgy* **2011**, *108*, 60–79. [CrossRef]
3. Santini, T.C.; Fey, M.V.; Gilkes, R. Experimental simulation of long term weathering in alkaline bauxite residue tailings. *Metals* **2015**, *5*, 1241–1261. [CrossRef]
4. Gräfe, M.; Klauber, C. Bauxite residue issues: IV. Old obstacles and new pathways for in situ residue bioremediation. *Hydrometallurgy* **2011**, *108*, 46–59. [CrossRef]
5. Higgins, D.; Curtin, T.; Burke, I.; Courtney, R. The potential for constructed wetland mechanisms to treat alkaline bauxite residue leachate: Carbonation and precipitate characterisation. *Environ. Sci. Pollut. Res.* **2018**, *25*, 29451–29458. [CrossRef]
6. Evans, K. The History, Challenges, and New Developments in the management and use of bauxite residue. *J. Sustain. Metall.* **2016**, *2*, 316–331. [CrossRef]
7. Willan, M.; Ghataora, G. Management of bauxite residue in a temperate climate using mud-farming techniques. In Proceedings of the 18th International Seminar on Paste and Thickened Tailings, Australian Centre for Geomechanics, Perth, Australia, 5–7 May 2015; pp. 209–222.
8. Kinnarinen, T.; Lubieniecki, B.; Holliday, L.; Helsto, J.-J.; Häkkinen, A. Enabling safe dry cake disposal of bauxite residue by deliquoring and washing with a membrane filter press. *Waste Manag. Res.* **2015**, *33*, 258–266. [CrossRef]
9. Kaußen, F.M.; Friedrich, B. Methods for alkaline recovery of aluminum from bauxite residue. *J. Sustain. Metall.* **2016**, *2*, 353–364. [CrossRef]
10. Doucet, J.; Paradis, R. Thickening/mud stacking technology—An environmental approach to residue management. In Proceedings of the Thirteenth International Seminar on Paste and Thickened Tailings, Australian Centre for Geomechanics, Toronto, ON, Canada, 3–6 May 2010; 2010; pp. 3–21.
11. Cooling, D.J. Improving the sustainability of residue management practices-Alcoa World Alumina Australia. In *Paste and Thickened Tailings: A Guide, Australian Centre for Geomechanics, Perth, Australia*; Australian Centre for Geomechanics: Perth, Australia, 2007; pp. 3–16.
12. Paramguru, R.K.; Rath, P.C.; Misra, V.N. Trends in red mud utilization—A review. *Miner. Process. Extr. Metall. Rev.* **2004**, *26*, 1–29. [CrossRef]
13. Kossoff, D.; Dubbin, W.; Alfredsson, M.; Edwards, S.; Macklin, M.; Hudson-Edwards, K. Mine tailings dams: Characteristics, failure, environmental impacts, and remediation. *Appl. Geochem.* **2014**, *51*, 229–245. [CrossRef]
14. Shaygan, M.; Baumgartl, T.; Arnold, S.; Reading, L.P. The effect of soil physical amendments on reclamation of a saline-sodic soil: Simulation of salt leaching using HYDRUS-1D. *Soil Res.* **2018**, *56*, 829. [CrossRef]
15. Rasouli, F.; Pouya, A.K.; Šimůnek, J. Modeling the effects of saline water use in wheat-cultivated lands using the UNSATCHEM model. *Irrig. Sci.* **2012**, *31*, 1009–1024. [CrossRef]
16. Shaygan, M.; Reading, L.P.; Arnold, S.; Baumgartl, T. Modeling the effect of soil physical amendments on reclamation and revegetation success of a saline-sodic soil in a semi-arid environment. *Arid Land Res. Manag.* **2018**, *32*, 379–406. [CrossRef]
17. Zeng, W.; Xu, C.; Wu, J.-W.; Huang, J. Soil salt leaching under different irrigation regimes: HYDRUS-1D modelling and analysis. *J. Arid Land* **2013**, *6*, 44–58. [CrossRef]

18. Gonçalves, M.; Simunek, J.; Ramos, T.; Martins, J.C.; Neves, M.J.; Pires, F.P. Multicomponent solute transport in soil lysimeters irrigated with waters of different quality. *Water Resour. Res.* **2006**, *42*. [CrossRef]
19. Newson, T.; Dyer, T.; Adam, C.; Sharp, S.; Dyer, T.D. Effect of structure on the geotechnical properties of bauxite residue. *J. Geotech. Geoenviron. Eng.* **2006**, *132*, 143–151. [CrossRef]
20. Smagin, A. Column-centrifugation method for determining water retention curves of soils and disperse sediments. *Eurasian Soil Sci.* **2012**, *45*, 416–422. [CrossRef]
21. Rashid, N.S.A.; Askari, M.; Tanaka, T.; Simunek, J.; van Genuchten, M.T. Inverse estimation of soil hydraulic properties under oil palm trees. *Geoderma* **2015**, *241*, 306–312. [CrossRef]
22. Ramos, T.; Gonçalves, M.; Martins, J.C.; Van Genuchten, M.T.; Pires, F.P. Estimation of soil hydraulic properties from numerical inversion of tension disk infiltrometer data. *Vadose Zone J.* **2006**, *5*, 684–696. [CrossRef]
23. Schwartz, R.C.; Evett, S.R. Estimating hydraulic properties of a fine-textured soil using a disc infiltrometer. *Soil Sci. Soc. Am. J.* **2002**, *66*, 1409–1423. [CrossRef]
24. Ventrella, D.; Losavio, N.; Vonella, A.; Leij, F. Estimating hydraulic conductivity of a fine-textured soil using tension infiltrometry. *Geoderma* **2005**, *124*, 267–277. [CrossRef]
25. Lazarovitch, N.; Ben-Gal, A.; Šimunek, J.; Shani, U. Uniqueness of soil hydraulic parameters determined by a combined wooding inverse approach. *Soil Sci. Soc. Am. J.* **2007**, *71*, 860–865. [CrossRef]
26. Botula, Y.-D.; Van Ranst, E.; Cornelis, W.M. Pedotransfer functions to predict water retention for soils of the humid tropics: A review. *Rev. Bras. Cienc. Solo* **2014**, *38*, 679–698. [CrossRef]
27. Shaygan, M.; Reading, L.P.; Baumgartl, T. Effect of physical amendments on salt leaching characteristics for reclamation. *Geoderma* **2017**, *292*, 96–110. [CrossRef]
28. Van Genuchten, M.T. A closed-form equation for predicting the hydraulic conductivity of unsaturated soils. *Soil Sci. Soc. Am. J.* **1980**, *44*, 892–898. [CrossRef]
29. Van Genuchten, M.T.; Leij, F.J.; Yates, S.R. *The RETC Code for Quantifying the Hydraulic Functions of Unsaturated Soils*; Version 1.0, EPA Report 600/2-91/065; US Salinity Laboratory, USDA-ARS: Riverside, CA, USA, 1991.
30. Klute, A.; Dirksen, C. Hydraulic conductivity and diffusivity: Laboratory methods. In *Methods of Soil Analysis-Physical and Mineralogical Methods*; Klute, A., Ed.; American Society of Agronomy: Madison, WI, USA, 1982; Volume 2, pp. 687–734.
31. Marshall, T.J.; Holmes, J.W.; Rose, C.W. *Soil Physics*; Cambridge University Press: New York, NY, USA, 1996.
32. Assouline, S.; Tessier, D.; Tavares-Filho, J. Effect of compaction on soil physical and hydraulic properties: Experimental results and modeling. *Soil Sci. Soc. Am. J.* **1997**, *61*, 390. [CrossRef]
33. Zhang, S.; Grip, H.; Lövdahl, L. Effect of soil compaction on hydraulic properties of two loess soils in China. *Soil Tillage Res.* **2006**, *90*, 117–125. [CrossRef]
34. Šimůnek, J.; Šejna, M.; Saito, H.; Sakai, M.; van Genuchten, M. *The Hydrus-1D Software Package for Simulating the Movement of Water, Heat, and Multiple Solutes in Variably Saturated Media*; Version 4.16; Department of Environmental Sciences, University of California Riverside: Riverside, CA, USA, 2013; p. 340.
35. Šimunek, J.; Van Genuchten, M.T.; Wendroth, O. Parameter estimation analysis of the evaporation method for determining soil hydraulic properties. *Soil Sci. Soc. Am. J.* **1998**, *62*, 894–905. [CrossRef]
36. Šimůnek, J.; Šejna, M.; Saito, H.; Sakai, M.; van Genuchten, M.T. *The HYDRUS-1D Software Package for Simulating the Movement of Water, Heat, and Multiple Solutes in Variably Saturated Media*; Version 4.0, Hydrus Software; Department of Environmental Sciences, University of California: Riverside, CA, USA, 2008.
37. Saso, J.K.; Parkin, G.W.; Drury, C.F.; Lauzon, J.D.; Reynolds, W.D. Chloride leaching in two Ontario soils: Measurement and prediction using HYDRUS-1D. *Can. J. Soil Sci.* **2012**, *92*, 285–296. [CrossRef]
38. LeGates, D.R.; McCabe, G.J. Evaluating the use of "goodness-of-fit" measures in hydrologic and hydroclimatic model validation. *Water Resour. Res* **1999**, *35*, 233–241. [CrossRef]
39. Nash, J.; Sutcliffe, J.V. River flow forecasting through conceptual models part I—A discussion of principles. *J. Hydrol.* **1970**, *10*, 282–290. [CrossRef]
40. Willmott, C.J. On the validation of models. *Phys. Geogr.* **1981**, *2*, 184–194. [CrossRef]
41. Ket, P.; Oeurng, C.; Degré, A. Estimating soil water retention curve by inverse modelling from combination of in situ dynamic soil water content and soil potential data. *Soil Syst.* **2018**, *2*, 55. [CrossRef]
42. Schwartz, R.C.; Evett, S.R. Conjunctive use of tension infiltrometry and time-domain reflectometry for inverse estimation of soil hydraulic properties. *Vadose Zone J.* **2003**, *2*, 530–538. [CrossRef]

43. Abbasi, F.; Simunek, J.; Feyen, J.; van Genuchten, M.T.; Shouse, P.J. Simultaneous inverse estimation of soil hydraulic and solute transport parameters from transient field experiments: Homogeneous soil. *Trans. ASAE* **2003**, *46*, 1085. [CrossRef]
44. Abbasi, F.; Feyen, J.; Van Genuchten, M.; Van Genuchten, M.T. Two-dimensional simulation of water flow and solute transport below furrows: Model calibration and validation. *J. Hydrol.* **2004**, *290*, 63–79. [CrossRef]
45. Shaygan, M.; Baumgartl, T. Simulation of the effect of climate variability on reclamation success of brine-affected soil in semi-arid environments. *Sustainability* **2020**, *12*, 371. [CrossRef]
46. Schwartz, M.O.; Schippers, A.; Hahn, L. Hydrochemical models of the sulphidic tailings dumps at Matchless (Namibia) and Selebi-Phikwe (Botswana). *Environ. Earth Sci.* **2005**, *49*, 504–510. [CrossRef]
47. Blanco, A.; Lloret, A.; Valhondo, C.; Olivella, S. Thermo-hydraulic behaviour of the vadose zone in sulphide tailings at Iberian Pyrite Belt: Waste characterization, monitoring and modelling. *Eng. Geol.* **2013**, *165*, 154–170. [CrossRef]
48. Dawood, I.; Aubertin, M. Effect of dense material layers on unsaturated water flow inside a large waste rock pile: A numerical investigation. *Mine Water Environ.* **2013**, *33*, 24–38. [CrossRef]
49. Fala, O.; Molson, J.; Aubertin, M.; Bussiere, B. Numerical modelling of flow and capillary barrier effects in unsaturated waste rock piles. *Mine Water Environ.* **2005**, *24*, 172–185. [CrossRef]
50. Hadi, H.N.; Luo, M.K.; Li, S. Assessment of unsaturated flow for a large coal mine waste rock pile. *Adv. Mater. Res.* **2014**, *955*, 1179–1183. [CrossRef]
51. Wissmeier, L.; Barry, D.; Phillips, I.R. Predictive hydrogeochemical modelling of bauxite residue sand in field conditions. *J. Hazard. Mater.* **2011**, *191*, 306–324. [CrossRef] [PubMed]
52. Fredlund, D.G.; Morgenstern, N.R.; Widger, R.A. The shear strength of unsaturated soils. *Can. Geotech. J.* **1978**, *15*, 313–321. [CrossRef]